# Performance Analysis and Optimization of ISAC Vehicular Networks with 360° Radar Detection

Like Wang\*, Yue Zhang\*, Hangguan Shan\*, Chen Chen<sup>†</sup>, Fen Hou<sup>‡</sup>, Huma Ghafoor<sup>§</sup>, and Yu Cheng<sup>¶</sup>
\*College of Information Science and Electronic Engineering, Zhejiang University, Hangzhou, China

<sup>†</sup>School of Telecommunication Engineering, Xidian University, Xi'an, China

<sup>‡</sup>Department of Electrical and Computer Engineering, University of Macau, Macau, China

<sup>§</sup>School of Electrical Engineering and Computer Science, National University of Sciences and Technology, Islamabad, Pakistan

¶Department of Electrical and Computer Engineering, Illinois Institute of Technology, Chicago, USA

Abstract—To alleviate the shortage of wireless spectrum for vehicular communications, integrated sensing and communication (ISAC) technology is expected to be applied to vehicular networks. In this paper, we design a dual-beam ISAC scheme that allows 360° radar detection and directional communication simultaneously. We then develop a stochastic geometry-based performance analytical framework to evaluate both sensing and communication performance of the dual-beam ISAC vehicular network. The detection probability and communication coverage probability are modeled by capturing the impact of both the incident and reflected interference. Furthermore, to improve the sensing performance of 360° radar detection while guaranteeing communication performance, we study two power allocation optimization problems. Simulation results not only validate the accuracy of the proposed analytical models, but also show the advantages of the proposed power allocation schemes in improving average detection probability.

#### I. Introduction

Autonomous vehicles constantly sense the surrounding environment via radar and other sensors, and the sensed data can be shared with other vehicles by communication technologies, improving driving safety. Instead of having two separate systems, developing integrated sensing and communication (ISAC) technology to integrate the two functions into one can not only achieve the benefits of reduced cost, size and weight of the hardware equipment and better spectrum efficiency, but also benefit by sharing information mutually, e.g., the sensed information can be used to assist beamforming, and the communication can help radar reduce interference [1].

However, the ISAC system needs to meet various requirements to enable simultaneous sensing and communication. The ISAC system is expected to provide a high data rate for communication and a high resolution for sensing. Thus, the millimeter wave (mmWave) is more competent than the sub-6G band for the ISAC system due to its large bandwidth [2]. One fundamental challenge in ISAC is that sensing requires time-varying scanning beams, while communication requires accurately pointed beams to overcome the large propagation

The work was supported by the Zhejiang Provincial Natural Science Foundation of China under Grant LR23F010006, the National Natural Science Foundation of China under Grants U21A20456, U21B2029, and 62027805, the open research project program funded by the Science and Technology Development Fund (SKL-IOTSC(UM)-2024-2026) and the State Key Laboratory of Internet of Things for Smart City (University of Macau) (Ref. No.: SKL-IoTSC(UM)-2024-2026/ORP/GA01/2023), and the University of Macau (Project No. MYRG-GRG2023-00200-FST and MYRG2022-00242-FST).

loss. While many sensing implementations [3–5] are limited to the direction of communication signals, the multibeam framework in [6] is proposed to achieve 360° radar detection and directional communication.

Introducing sensing capability to vehicular networks requires us to consider simultaneous communication and sensing functions design. To this aim, developing tractable models that can evaluate communication and sensing performance is of critical importance. Stochastic geometry has been applied widely to analyze the performance of vehicular networks, but most works are limited to only the communication systems [7, 8] or radar systems [9–11]. Although [12] evaluates both functions' performance of ISAC vehicular networks, the directions of sensing and communication are both limited to the front and only the incident interference is considered. However, reflected interference in mmWave networks is not negligible [11]. Inspired by the studies above, we aim to fill the gap by proposing an analytical model for the dual-beam ISAC vehicular network supporting 360° radar detection and directional communication capturing the impact of both the incident and complex reflected interference.

In this paper, we first design a dual-beam ISAC scheme supporting 360° radar detection and directional communication for vehicular networks. Then, adopting the Matérn hard-core process (MHCP) to model the vehicle positions, we propose a stochastic geometry-based performance analytical framework to evaluate the sensing and communication performance of the networks by capturing the incident and complex reflected interference in a dual-direction and two-lane scenario. Then, to improve the sensing performance of 360° radar detection while guaranteeing communication performance, we study two power allocation optimization problems. Finally, Monte Carlo simulations are conducted to validate the analytical results. Simulation results also verify the advantages of the power allocation schemes in average detection probability (DP) enhancement.

# II. SYSTEM MODEL

In this section, we introduce the research scenario, the power allocation setting, the channel model, and the signal model of the ISAC vehicular network.

# A. Research Scenario

We consider a dual-direction and two-lane scenario as shown in Fig. 1, with the width of each lane equal to l. On

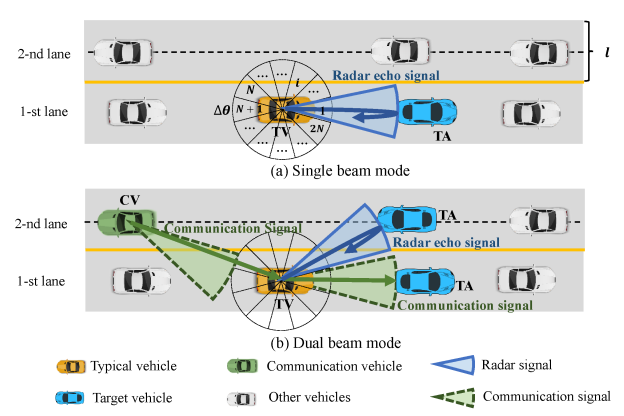


Fig. 1. Illustration of the proposed ISAC equipment working mode. each lane, the locations of vehicles are modeled by a one-dimensional (1D) MHCP of type II with the same density  $\lambda_h = [1 - \exp(-2\lambda_p d_h)]/2d_h$  [8], which is generated from a 1D Poisson point process (PPP) with density  $\lambda_p$ . Here,  $d_h$  is the hard-core distance, i.e., the minimum separation between two proximate vehicles. We denote the sets of the vehicles on the first and second lane as  $\Phi_s$  and  $\Phi_o$ , respectively. Without loss of generality, we focus on the vehicle located at the origin and name it the typical vehicle (TV), which is considered a receiver receiving its own radar echo signals or communication signals from communication vehicles (CVs). We assume that radio resources are allocated to each vehicle randomly at the medium access control layer and the probability of a vehicle using the same time-frequency resource as the TV is  $\varepsilon$ .

The ISAC devices on the vehicles have two working modes: the single-beam mode and the dual-beam mode [6]. We assume that the beamwidth is  $\theta$ , then there are  $2N=2\pi/\theta$  sectors for a 360° radar. The sectors are numbered from 1 to 2N in the counterclockwise direction starting from the forward sector. At first, a vehicle is in the single-beam mode and subsequently detects whether there are other vehicles around it, to achieve  $360^{\circ}$  radar sensing. If a vehicle is detected in a certain sector, the working mode is switched to the dual-beam mode, i.e., one beam used for detecting the next sector and the other beam used for communicating with the detected vehicle if required. B. Power Allocation Setting

We denote  $P_{\rm r}(i)$  as the radar signal transmission power of sector  $i \in \{1, 2, \ldots, 2N\}$ . Here, we consider that, if the radar signal is sent in the forward sector, i.e., i=1, then  $P_{\rm r}(i)=P_{\rm rf}$ , otherwise  $P_{\rm r}(i)=P_{\rm rs}$ . Notice that in general, we have  $P_{\rm rf} \geq P_{\rm rs}$ . How to appropriately set  $P_{\rm r}(i)$  is to be studied in Section IV. To ensure the communication performance of vehicles in all sectors, we set the communication power of each sector to be the same, i.e.,  $P_{\rm c}(i)=P_{\rm c}$ ,  $i\in\{1,2,\ldots,2N\}$ .

Assume that  $P_{T,\mathbf{x}_T}(i)$  is the transmission power of vehicle at coordinate  $\mathbf{x}_T$  in sector i using the same time-frequency resource as the TV, with T = "r", "c", or "no", indicating transmitting radar signals, transmitting communication signals, or not transmitting signals, respectively. The probability of vehicle  $\mathbf{x}_T$  transmitting radar signal and communication signal in sector i using the same time-frequency resource as the TV

is  $\mathbb{P}[P_{\mathrm{T},\mathbf{x}_{\mathrm{T}}}(i) = P_{\mathrm{r}}(i)] = \varepsilon \frac{\theta}{2\pi}$  and  $\mathbb{P}[P_{\mathrm{T},\mathbf{x}_{\mathrm{T}}}(i) = P_{\mathrm{c}}(i)] = \varepsilon \frac{\theta}{2\pi} P_{\mathrm{d},i}$ , respectively, with  $P_{\mathrm{d},i}$  being the detection probability that a vehicle detects a target in sector i.

## C. Channel Model

- 1) Small-Scale Fading: The mmWave radar and communication channels are both modeled as the Nakagami-m fading with shape parameter m [10]. We denote  $h_{\mathbf{x}_T}$  and  $h_{\mathbf{x}_T,\mathbf{x}_R}$  as the channel gain of the link from vehicle  $\mathbf{x}_T$  to the TV, and the link from vehicle  $\mathbf{x}_T$  to the TV via the reflection of vehicle  $\mathbf{x}_R$ , respectively, where  $\mathbf{x}_R$  is the coordinate of the reflector vehicle. The cumulative distribution function (CDF) of the channel gain can be expressed as  $F_h(x) = \frac{\Gamma_L(m,mx)}{\Gamma(m)}$ , where we denote h as channel gain for simplicity, and  $\Gamma_L(m,mx) = \int_0^{mx} t^{m-1} \mathrm{e}^{-t} \mathrm{d}t$  is the lower incomplete Gamma function [13].

  2) Large-Scale Fading: For the incident signals, the
- 2) Large-Scale Fading: For the incident signals, the path loss model can be expressed as  $L_{\rm inc}(d_{\rm inc})=(4\pi)^{-2}G_{\rm T}G_{\rm R}(c/f_c)^2d_{\rm inc}^{-\alpha}$  [12], where  $G_{\rm T}$  and  $G_{\rm R}$  are the transmitting and receiving main beam gain, respectively,  $\alpha$  is the path loss exponent, c is the light speed,  $f_c$  is the carrier frequency, and  $d_{\rm inc}$  is the distance between the transmitter and the receiver. As the signal power after multiple reflections is severely attenuated, only the single reflected signals are considered in this work. The path loss model of reflected signals is  $L_{\rm ref}(d_{\rm ref,1},d_{\rm ref,2})=(4\pi)^{-3}G_{\rm T}\sigma G_{\rm R}(c/f_c)^2d_{\rm ref,1}^{-\alpha}d_{\rm ref,2}^{-\alpha}$  [9], where  $\sigma$  is the average radar cross-section (RCS) of vehicles,  $d_{\rm ref,1}$  ( $d_{\rm ref,2}$ ) is the distance between the transmitter (receiver) and the reflector vehicle.

# D. Signal Model

- 1) Radar Echo Signal: The power of the radar echo signal received by the TV in sector i is  $S_{\mathrm{r},i}(d_{\mathrm{r}}) = P_{\mathrm{r}}(i)h_{\mathbf{x}_{\mathrm{TV}},\mathbf{x}_{\mathrm{TA}}}L_{\mathrm{ref}}(d_{\mathrm{r}},d_{\mathrm{r}})$ , where  $d_{\mathrm{r}}$  is the distance between the TV and the target vehicle (TA). Here, we consider the TA as the nearest vehicle in the sensing area of the TV.  $\mathbf{x}_{\mathrm{TV}} = (0,0)$  is the TV's coordinate,  $\mathbf{x}_{\mathrm{TA}}$  is the TA's coordinate, and  $||\mathbf{x}_{\mathrm{TA}}|| = d_{\mathrm{r}}$  denotes the Euclidean distance between the origin and  $\mathbf{x}_{\mathrm{TA}}$ .
- 2) Communication Signal: Assuming that the CV is  $d_c$  meters away from the TV, the power of the communication signal received by the TV in sector i is  $S_{c,i}(d_c) = P_c h_{\mathbf{x}_{CV}} L_{\text{inc}}(d_c)$ , where  $\mathbf{x}_{CV}$  is the CV's coordinate, and  $||\mathbf{x}_{CV}|| = d_c$ .

# III. INTERFERENCE ANALYSIS OF ISAC NETWORKS

In this section, we analyze the incident and reflected interference that the TV suffers from, based on which the network performance is to be characterized in the next section.

# A. Incident Interference

Assume that the TV receives the radar echo signal or communication signal in sector  $i \in \{1, 2, ..., N+1\}$ . Other sectors are not analyzed because of the dual-direction and two-lane road setting. As shown in Fig. 2, there are two cases of incident interference described as follows.

**Case 1:** As shown in Fig. 2(a), located in sector i's sensing area of the TV, the oncoming vehicle  $\mathbf{x}_{\mathrm{T}}$  sending signals in sector i may generate incident interference to the TV. Sector i's sensing area of the TV is the segment of the second lane covered by the TV's beam, denoted as  $S_i = {\mathbf{x} = (x, l)|x \in \mathbb{R}}$ 

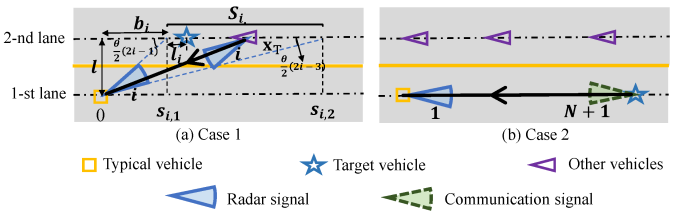


Fig. 2. Illustration of the incident interference.

 $\{s_{i,1},s_{i,2}\}\$ , where  $s_{i,1}=l/\mathrm{tan}[\frac{\theta}{2}(2i-1)]$  if  $1\leq i\leq N$ ,  $s_{i,1}=-\infty$  if i=N+1,  $s_{i,2}=+\infty$  if i=1, and  $s_{i,2}=-\infty$  $l/\tan[\frac{\theta}{2}(2i-3)]$  if  $2 \le i \le N+1$ . Then, the power of the interference from vehicles in  $\Phi_{o,i} = \{\mathbf{x} | \mathbf{x} \in S_i, \mathbf{x} \in \Phi_o\}, I_{1,i}^{\text{inc}},$ can be obtained as

$$I_{1,i}^{\text{inc}} = \sum_{\mathbf{x}_{\text{T}} \in \Phi_{\text{o},i}} P_{\text{T},\mathbf{x}_{\text{T}}}(i) h_{\mathbf{x}_{\text{T}}} L_{\text{inc}}(||\mathbf{x}_{\text{T}}||). \tag{1}$$

Case 2: As shown in Fig. 2(b), the TV sensing in sector i = 1 (N + 1) may be interfered by the TA, if the latter is transmitting signals in sector j = N + 1 (1) simultaneously. Then, the power of the interference from the TA,  $I_{2,i}^{\text{inc}}$ , satisfies

$$I_{2,i}^{\text{inc}} = P_{\text{T},\mathbf{x}_{\text{TA}}}(j)h_{\mathbf{x}_{\text{TA}}}L_{\text{inc}}(d_{\text{r}})$$
(2)

and  $I_{2,i}^{\text{inc}} = 0$  if  $i \in \{2, 3, ..., N\}$ .

## B. Reflected Interference

Next, we study the reflected interference sent by the interferers and reflected by other vehicles. Assume the TV receives the desired signal in sector  $i \in \{1, 2, ..., N+1\}$ . Next, we detail three cases of the reflected interference, shown in Fig. 3.

Case 1: As shown in Fig. 3(a), a vehicle  $\mathbf{x}_{\mathrm{T}}$  on the first lane sending signals in sector  $n \in \{1, 2, ..., N + 1\}$  may generate reflected interference to the TV through the reflection of a vehicle  $\mathbf{x}_{\mathrm{R}}$  located in sector i's sensing area of the TV. Let  $S_n^* = \{ \mathbf{x} = (x,0) | x_R - x \in (s_{n,1}, s_{n,2}) \}$  be the area that the signals of vehicle  $\mathbf{x}_T$  in sector n can reach vehicle  $\mathbf{x}_R$ . Here,  $x_{\rm R}$  is the horizontal coordinate of vehicle  $\mathbf{x}_{\rm R}$ ,  $s_{n,1}$  and  $s_{n,2}$ can be obtained similar to  $s_{i,1}$  and  $s_{i,2}$ . Then, the power of the interference from vehicles in  $\Phi_{s,n} = \{ \mathbf{x} | \mathbf{x} \in S_n^*, \mathbf{x} \in \Phi_s \},$ which is reflected by vehicles in  $\Phi_{o,i}$ , can be calculated as

$$I_{1,i}^{\text{ref}} = \sum_{\mathbf{x}_{R} \in \Phi_{o,i}} \sum_{n=1}^{N+1} \sum_{\mathbf{x}_{T} \in \Phi_{s,n}} \frac{P_{T,\mathbf{x}_{T}}(n) h_{\mathbf{x}_{T},\mathbf{x}_{R}}}{L_{\text{ref}}^{-1}(||\mathbf{x}_{T} - \mathbf{x}_{R}||, ||\mathbf{x}_{R}||)}.$$
 (3)

Case 2: As shown in Fig. 3(b), a vehicle  $\mathbf{x}_T$  that is sending signals in sector 1 (N + 1) on the second lane may also generate the reflected interference to the TV through the reflection of a vehicle  $\mathbf{x}_{\mathrm{R}}$  in front (behind) it. In this case,

the power of reflected interference 
$$I_{2,i}^{\text{ref}}$$
 can be calculated as
$$I_{2,i}^{\text{ref}} = \sum_{\mathbf{x}_{\text{R}} \in \Phi_{\text{o},i}} \frac{P_{\text{T},\mathbf{x}_{\text{T}}}(1)\mathbb{I}(x_{\text{R}} < 0) + P_{\text{T},\mathbf{x}_{\text{T}}}(N+1)\mathbb{I}(x_{\text{R}} > 0)}{L_{\text{ref}}^{-1}(v,||\mathbf{x}_{\text{R}}||)} h_{\mathbf{x}_{\text{T}},\mathbf{x}_{\text{R}}}$$
(4)

where v is the distance between the potential interferer and the reflector, with the probability density function (PDF)  $f_V(v)$ derived from Proposition 1 in [8], and the indicator function  $\mathbb{I}(X)$  equals 1 if event X occurs, otherwise equals 0. In (4), if  $x_{\rm R} < 0 \ (x_{\rm R} > 0)$ , the TV is only interfered by the oncoming vehicles that send signals in sector 1 (N+1).

Case 3: As shown in Fig. 3(c), if the TV is receiving radar signals in sector i = 1 (N+1), the TA as a reflector scatters the

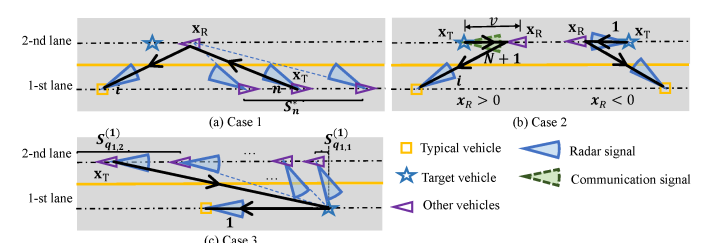


Fig. 3. Illustration of the reflected interference.

unwanted signals back to the TV, and the potential interferer  $\mathbf{x}_{\mathrm{T}} = (x_{\mathrm{T}}, l)$  is behind (in front of) the TA and on the second lane, i.e.,  $x_{\rm T} < x_{\rm TA}$   $(x_{\rm T} > x_{\rm TA})$ . We denote  $S_q^{(i)}$  as the area that the signals of vehicle  $\mathbf{x}_{\mathrm{T}}$  in sector  $q \in \{q_{i,1},...,q_{i,2}\}$  can reach vehicle  $\mathbf{x}_{\text{TA}}$ . If  $i=1, S_q^{(i)}=\{\mathbf{x}=(x,l)|x-x_{\text{TA}}\in$  $(s_{q,1}, s_{q,2}), x < x_{\text{TA}}$  with  $q_{i,1} = \lceil \frac{N}{2} \rceil + 1$  and  $q_{i,2} = N + 1$ . If i=N+1,  $S_q^{(i)}=\{\mathbf{x}=(x,l)|x-x_{\mathrm{TA}}\in(s_{q,1},s_{q,2}),x>x_{\mathrm{TA}}\}$  with  $q_{i,1}=1$  and  $q_{i,2}=N+1-\lceil\frac{N}{2}\rceil$ . Here,  $s_{q,1}$ and  $s_{q,2}$  can be obtained similar to  $s_{i,1}$  and  $s_{i,2}$ ,  $x_T$  is the horizontal coordinate of vehicle  $\mathbf{x}_{\mathrm{T}}$ , and  $\lceil \cdot \rceil$  represents round up. Then, if i=1 or N+1, the power of the interference from vehicles in  $\Phi_{\mathrm{o},q}^{(i)} = \{\mathbf{x} | \mathbf{x} \in S_q^{(i)}, \mathbf{x} \in \Phi_{\mathrm{o}}\}$ , can be obtained as  $I_{3,i}^{\mathrm{ref}} = \sum_{q=q_{i,1}} \sum_{\mathbf{x}_{\mathrm{T}} \in \Phi_{\mathrm{o},q}^{(i)}} \frac{P_{\mathrm{T},\mathbf{x}_{\mathrm{T}}}(q)h_{\mathbf{x}_{\mathrm{T}},\mathbf{x}_{\mathrm{TA}}}}{L_{\mathrm{ref}}^{-1}(||\mathbf{x}_{\mathrm{T}} - \mathbf{x}_{\mathrm{TA}}||,||\mathbf{x}_{\mathrm{TA}}||)}$ (5)

$$I_{3,i}^{\text{ref}} = \sum_{q=q_{i,1}} \sum_{\mathbf{x}_{\mathrm{T}} \in \Phi_{0,q}^{(i)}} \frac{P_{\mathrm{T},\mathbf{x}_{\mathrm{T}}}(q) h_{\mathbf{x}_{\mathrm{T}},\mathbf{x}_{\mathrm{TA}}}}{L_{\text{ref}}^{-1}(||\mathbf{x}_{\mathrm{T}} - \mathbf{x}_{\mathrm{TA}}||, ||\mathbf{x}_{\mathrm{TA}}||)}$$
(5)

and  $I_{3,i}^{\text{ref}} = 0$  if  $i \in \{2, 3, ..., N\}$ . Notice that, if the TV is receiving communication signals in sector 1 or N+1, we only need to replace  $\mathbf{x}_{TA}$  in the above equation with  $\mathbf{x}_{CV}$ .

#### IV. PERFORMANCE ANALYSIS AND OPTIMIZATION

In this section, we analyze the radar and communication performance of the vehicular networks, in terms of detection probability and communication coverage probability (CCP).

#### A. Detection Probability

We study the radar performance of the ISAC vehicular networks in terms of the detection probability [9], which is defined as the probability that the signal-to-interference-plusnoise ratio (SINR) of the radar echo received by the TV is no less than the radar SINR threshold  $\gamma_r$ . Then, the detection probability at detection distance  $d_r$  in sector i,  $P_{d,i}(d_r)$ , can be defined as

$$P_{\mathrm{d},i}(d_{\mathrm{r}}) = \mathbb{P}\left\{\frac{S_{\mathrm{r},i}(d_{\mathrm{r}})}{I_{\mathrm{r},i} + N_0 B} \ge \gamma_{\mathrm{r}}\right\}$$
(6)

where  $I_{\mathrm{r},i} = \sum_{k=1}^2 I_{k,i}^{\mathrm{inc}} + \sum_{k'=1}^3 I_{k',i}^{\mathrm{ref}}$  is the interference signal power at sector i of the radar receiver,  $N_0$  is the noise power spectral density, and B is the bandwidth. For  $I_{r,i}$ , we have the following lemma.

Lemma 1: The Laplace transform of the interference received by the TV in sector i,  $I_{r,i}$ , is given by:

$$\mathcal{L}_{I_{r,i}}(s) \approx \mathcal{L}_{I_{2,i}^{\text{inc}}}(s) \exp\left[-\lambda_h \int_{-\infty}^{+\infty} 1 - Y(x, s) dx\right]$$
(7)

where the Laplace transform of incident interference  $I_{2,i}^{\text{inc}}$  is

where the Laplace transform of incident interference 
$$I_{2,i}$$
 is
$$\mathcal{L}_{I_{2,i}^{\text{inc}}}(s) = \begin{cases}
1 - \varepsilon \frac{\theta}{2\pi} \left( 1 + P_{\text{d},j} \right) + \varepsilon \frac{\theta}{2\pi} \mathcal{L}_h(sP_{\text{r}}(j)L_{\text{inc}}(d_{\text{r}})) + \varepsilon \frac{\theta}{2\pi} P_{\text{d},j} \mathcal{L}_h(sP_{\text{c}}L_{\text{inc}}(d_{\text{r}})), i = 1 \text{ or } N + 1 \\
1, \text{ otherwise}
\end{cases} \tag{8}$$

$$\zeta_{1,i}^{\text{ref}} = \prod_{n=1}^{N+1} \exp\left\{-\varepsilon \frac{\theta}{2\pi} \lambda_{h} \int_{s_{n,1}}^{s_{n,2}} \left[1 + P_{d,n} - \mathcal{L}_{h} \left(sP_{r}(n)L_{\text{ref}}(G_{l}(r), G_{l}(x))\right) - P_{d,n} \mathcal{L}_{h} \left(sP_{c}L_{\text{ref}}(G_{l}(r), G_{l}(x))\right)\right] dr\right\} \tag{11}$$

$$\zeta_{2,i}^{\text{ref}} = \left\{\varepsilon \frac{\theta}{2\pi} \int_{0}^{+\infty} \left[\mathcal{L}_{h} \left(sP_{r}(1)L_{\text{ref}}(v, G_{l}(x))\right) + P_{d,1} \mathcal{L}_{h} \left(sP_{c}L_{\text{ref}}(v, G_{l}(x))\right)\right] f_{V}(v) dv + 1 - \varepsilon \frac{\theta}{2\pi} \left(1 + P_{d,1}\right)\right\} \mathbb{I}(x < 0) + \left\{\varepsilon \frac{\theta}{2\pi} \int_{0}^{+\infty} \left[\mathcal{L}_{h} \left(sP_{r}(N+1)L_{\text{ref}}(v, G_{l}(x))\right) + P_{d,N+1} \mathcal{L}_{h} \left(sP_{c}L_{\text{ref}}(v, G_{l}(x))\right)\right] f_{V}(v) dv + 1 - \varepsilon \frac{\theta}{2\pi} \left(1 + P_{d,N+1}\right)\right\} \mathbb{I}(x > 0)$$

with  $\mathcal{L}_h(w) = [m/(m+w)]^m$ , j = N+1 if i = 1, j = 1 if i = N + 1; and Y(x, s) can be expressed as

$$Y(x,s) = \begin{cases} \zeta_{1,i}^{\text{inc}} \prod_{k'=1}^{3} \zeta_{k',i}^{\text{ref}}, s_{i,1} < x < s_{i,2} \\ \zeta_{3,i}^{\text{ref}}, x \ge s_{i,1} \text{ or } x \le s_{i,2} \end{cases}$$
(9)

with  $\zeta_{1,i}^{\mathrm{inc}}$  and  $\zeta_{k',i}^{\mathrm{ref}}$  ( $k' \in \{1,2,3\}$ ) being the Laplace transform of  $I_{1,i}^{\mathrm{inc}}$  and  $I_{k',i}^{\mathrm{ref}}$  given set  $\Phi_{\mathrm{o}}$ , respectively. Here,  $\zeta_{1,i}^{\mathrm{inc}}$  satisfies  $\zeta_{1,i}^{\mathrm{inc}} = 1 - \varepsilon \frac{\theta}{2\pi} (1 + P_{\mathrm{d},i}) + \varepsilon \frac{\theta}{2\pi} \mathcal{L}_h(sP_{\mathrm{r}}(i)L_{\mathrm{inc}}(G_l(x))) +$ 

$$\zeta_{1,i}^{\text{inc}} = 1 - \varepsilon \frac{\theta}{2\pi} (1 + P_{d,i}) + \varepsilon \frac{\theta}{2\pi} \mathcal{L}_h(sP_r(i)L_{\text{inc}}(G_l(x))) + \varepsilon \frac{\theta}{2\pi} P_{d,i} \mathcal{L}_h\left(sP_cL_{\text{inc}}(G_l(x))\right)$$
(10)

with  $G_l(x)=\sqrt{x^2+l^2};\;\zeta_{1,i}^{\rm ref}$  and  $\zeta_{2,i}^{\rm ref}$  are given in (11) and (12) at the top of this page, in which  $r = x_R - x_T$ ; and  $\zeta_{3,i}^{ref}$ 

$$\zeta_{3,i}^{\text{ref}} = \begin{cases}
\prod_{q=q_{i,1}}^{q_{i,2}} \left[ \varepsilon \frac{\theta}{2\pi} \mathcal{L}_h(sP_{r}(q)L_{\text{ref}}(G_l(x-x_{\text{TA}}), d_r)) + \varepsilon \frac{\theta}{2\pi} P_{d,q} \mathcal{L}_h(sP_{c}L_{\text{ref}}(G_l(x-x_{\text{TA}}), d_r)) - \varepsilon \frac{\theta}{2\pi} (1 + P_{d,q}) \right] \mathbb{I}(\mathbf{x} \in S_q^{(i)}) + 1, i = 1 \text{ or } N + 1
\end{cases}$$
(13)

*Proof:* The Laplace transform of the interference received by the TV in sector i,  $I_{r,i}$ , can be calculated as follows

$$\mathcal{L}_{I_{\mathbf{r},i}}(s) \stackrel{\text{(a)}}{=} \mathbb{E}_{P_{\mathbf{T}},h} \left[ e^{-sI_{2,i}^{\mathrm{inc}}} \right] \mathbb{E} \left[ e^{-s\left(I_{1,i}^{\mathrm{inc}} + \sum_{k'=1}^{3} I_{k',i}^{\mathrm{ref}}\right)} \right]$$

$$\stackrel{\text{(b)}}{\approx} \mathcal{L}_{I_{2,i}^{\mathrm{inc}}}(s) \mathbb{E}_{\Phi_{0}} \left\{ \mathbb{E}_{P_{\mathbf{T}},h} \left[ e^{-sI_{3,i}^{\mathrm{ref}}} \right] \prod_{\mathbf{x}_{\mathbf{T}} \in \Phi_{0,i}} \mathbb{E}_{P_{\mathbf{T}},h} \left[ e^{-sI_{1,i}^{\mathrm{inc}} + \Phi_{0}} \right] \right]$$

$$\stackrel{\text{(b)}}{\approx} \mathcal{L}_{I_{2,i}^{\mathrm{inc}}}(s) \mathbb{E}_{\Phi_{0}} \left\{ \mathbb{E}_{P_{\mathbf{T}},h} \left[ e^{-sI_{1,i}^{\mathrm{ref}} + \Phi_{0}} \right] \mathbb{E}_{P_{\mathbf{T}},h} \left[ e^{-sI_{1,i}^{\mathrm{ref}} + \Phi_{0}} \right] \right\}$$

$$\stackrel{\text{(b)}}{\approx} \mathcal{L}_{I_{2,i}^{\mathrm{inc}}}(s) \mathbb{E}_{\Phi_{0}} \left\{ \mathbb{E}_{P_{\mathbf{T}},h} \left[ e^{-sI_{1,i}^{\mathrm{ref}} + \Phi_{0}} \right] \mathbb{E}_{P_{\mathbf{T}},h} \left[ e^{-sI_{2,i}^{\mathrm{ref}} + \Phi_{0}} \right] \right\}$$

where  $I_{1,i|\Phi_o}^{\rm inc}$ ,  $I_{1,i|\Phi_o}^{\rm ref}$ , and  $I_{2,i|\Phi_o}^{\rm ref}$  are  $I_{1,i}^{\rm inc}$ ,  $I_{1,i}^{\rm ref}$ , and  $I_{2,i}^{\rm ref}$  given set  $\Phi_0$ , respectively. (a) holds because  $I_{2,i}^{\text{inc}}$  is independent of other interference. If i=1 or N+1, vehicle  $\mathbf{x}_{\mathrm{T}}$  in  $I_{2,i}^{\mathrm{ref}}$  and  $I_{3,i}^{\text{ref}}$  maybe the same vehicle, i.e.,  $I_{2,i}^{\text{ref}}$  and  $I_{3,i}^{\text{ref}}$  are correlated. But the probability of this event is small. So, to facilitate the analysis, we assume that they are independent. Then, (b) can be obtained by the above assumption and the fact that the small-scale fading of each interfering link is independent.

Next, we calculate the Laplace transform of  $I_{2i}^{\text{inc}}$ . If i=1or N+1,  $\mathcal{L}_{I_{2,\delta}^{\text{inc}}}(s)$  can be obtained as

$$\mathcal{L}_{I_{2,i}^{\text{inc}}}(s) \stackrel{\text{(c)}}{=} \mathbb{E}_{P_{\text{T}}} [\mathcal{L}_{h}(sP_{\text{T},\mathbf{x}_{\text{TA}}}(j)L_{\text{inc}}(d_{\text{r}}))]$$

$$\stackrel{\text{(d)}}{=} 1 - \varepsilon \frac{\theta}{2\pi} (1 + P_{\text{d},j}) + \varepsilon \frac{\theta}{2\pi} \mathcal{L}_{h}(sP_{\text{r}}(j)L_{\text{inc}}(d_{\text{r}})) + \qquad (15)$$

$$\varepsilon \frac{\theta}{2\pi} P_{\text{d},j} \mathcal{L}_{h}(sP_{\text{c}}L_{\text{inc}}(d_{\text{r}}))$$

where (c) follows the PDF of the Nakagami-m channel gain from [13], and (d) can be obtained by averaging on  $P_{T,\mathbf{x}_{TA}}(j)$ . Otherwise,  $I_{2,i}^{\text{inc}} = 0$  and  $\mathcal{L}_{I_{2,i}^{\text{inc}}}(s) = 1$ , for  $i \in \{2, 3, ..., N\}$ .

Then, the second item in (14) can be expressed as

$$\mathbb{E}_{P_{\mathbf{T}},h}\left[e^{-sI_{3,i}^{\mathrm{ref}}}\right] = \prod_{\mathbf{x} \in \Phi_{\mathbf{O}}} \mathbb{E}_{P_{\mathbf{T}},h}\left[e^{-sI_{3,i}^{\mathrm{ref}}}\right] = \prod_{\mathbf{x} \in \Phi_{\mathbf{O}}} \zeta_{3,i}^{\mathrm{ref}} \qquad (16)$$

 $\mathbb{E}_{P_{\mathbf{T}},h}\left[\mathrm{e}^{-sI_{3,i}^{\mathrm{ref}}}\right] = \prod_{\mathbf{x}\in\Phi_{o}} \mathbb{E}_{P_{\mathbf{T}},h}\left[\mathrm{e}^{-sI_{3,i}^{\mathrm{ref}}}\right] = \prod_{\mathbf{x}\in\Phi_{o}} \zeta_{3,i}^{\mathrm{ref}} \qquad (16)$  where  $I_{3,i}^{\mathrm{ref}}|_{\Phi_{o}} = \prod_{q=q_{i,1}}^{q_{i,2}} \frac{P_{\mathbf{T},\mathbf{x}}(q)h_{\mathbf{x},\mathbf{x}_{\mathbf{T}A}}\mathbb{I}(\mathbf{x}\in S_{q}^{(i)})}{L_{\mathrm{ref}}^{-1}(||\mathbf{x}-\mathbf{x}_{\mathbf{T}A}||,||\mathbf{x}_{\mathbf{T}A}||)}$ , and  $\zeta_{3,i}^{\mathrm{ref}}$  is given in (13). For  $\zeta_{1,i}^{\mathrm{inc}}$ , we can obtain it in the same way as (c) and (d). For  $\zeta_{1,i}^{\text{ref}}$ , it satisfies

$$\zeta_{1,i}^{\text{ref}} \stackrel{\text{(e)}}{\approx} \prod_{n=1}^{N+1} \exp\left\{-\lambda_{h} \int_{s_{n,1}}^{s_{n,2}} \left\{1-\right] \\
\mathbb{E}_{P_{\text{T}},h} \left[ \exp\left(-s \frac{P_{\text{T},\mathbf{x}_{\text{T}}}(n) h_{\mathbf{x}_{\text{T}},\mathbf{x}_{\text{R}}}}{L_{\text{ref}}^{-1}(G_{l}(r), ||\mathbf{x}_{\text{R}}||)}\right) \right] \right\} dr \right\}$$
(17)

where (e) is obtained by approximating the MHCP with the homogeneous PPP and applying the probability generating functional of a PPP [11]. Then  $\zeta_{1,i}^{\text{ref}}$  in (11) is derived following from (c) and (d). And  $\zeta_{2,i}^{\text{ref}}$  in (12) can be obtained similar to  $\zeta_{1,i}^{\text{inc}}$ . Finally, as  $\Phi_{0,i} \in \Phi_0$ , Y(x,s) in (9) can be obtained, and (14) can be expressed as

$$\mathcal{L}_{I_{r,i}}(s) = \mathcal{L}_{I_{2,i}^{\text{inc}}}(s) \mathbb{E}_{\Phi_{o}} \left\{ \prod_{\mathbf{x} \in \Phi_{o}} Y(x,s) \right\}$$

$$\approx \mathcal{L}_{I_{2,i}^{\text{inc}}}(s) \exp \left\{ -\lambda_{h} \int_{-\infty}^{+\infty} 1 - Y(x,s) dx \right\}.$$

$$(18)$$

Next, we introduce several concepts needed later. As shown in Fig. 2, the edge of the TV's sector i intersects the center line of the second road at two points. If  $i = 2, 3, ..., N, l_i \in$  $(l_{i,1}, l_{i,2})$  represents the distance between the TA and the point close to the TV with  $l_{i,1} = 0$  and  $l_{i,2} = s_{i,2} - s_{i,1}$ . If i = 1or N+1,  $l_i$  represents the distance between the TA and the TV with  $l_{i,1} = d_h$  and  $l_{i,2} = +\infty$ . It is obvious that, if i = 1or N+1,  $d_{\rm r}=l_i$ , if i=2,3,...,N,  $d_{\rm r}=\sqrt{l^2+(b_i+l_i)^2}$  with  $b_i=\min\{|s_{i,1}|,|s_{i,2}|,\frac{s_{i,1}+s_{i,2}}{2}\}$  denoting the horizontal distance of the point close to the TV. The PDF of  $l_i$ ,  $f_{L_i}(l_i)$ ,

$$f_{L_i}(l_i) = \begin{cases} 2\lambda_h \exp(-2\lambda_h l_i), i = N/2 + 1 \in \mathbb{Z} \\ f_V(l_i), i = 1 \text{ or } N + 1 \\ \lambda_h \exp(-\lambda_h l_i), \text{ otherwise} \end{cases}$$
(19)

in which  $\mathbb{Z}$  represents the integer set.

Lemma 2: The detection probability that a vehicle detects a target in sector i,  $P_{\mathrm{d},i}$  has the following lower bound

$$P_{d,i} \ge P_{d,i}[d_r(\bar{l}_i)] \int_{l_{i,1}}^{l_i} f_{L_i}(l_i) dl_i$$
 (20)

where  $\bar{l}_i = \int_{l_{i,1}}^{l_{i,2}} l_i f_{L_i}(l_i) \mathrm{d}l_i$  is the average of  $l_i$ . *Proof:* According to the definition of  $P_{\mathrm{d},i}$ , we have

$$P_{d,i} = \int_{l_{i,1}}^{l_{i,2}} P_{d,i}(d_{r}(l_{i})) f_{L_{i}}(l_{i}) dl_{i}$$

$$\stackrel{(f)}{\geq} \int_{l_{i,1}}^{\bar{l}_{i}} P_{d,i}(d_{r}(l_{i})) f_{L_{i}}(l_{i}) dl_{i} \stackrel{(g)}{\geq} P_{d,i}(d_{r}(\bar{l}_{i})) \int_{l_{i,1}}^{\bar{l}_{i}} f_{L_{i}}(l_{i}) dl_{i}$$
(21)

where (f) is obtained because  $P_{d,i}(d_r)f_{L_i}(l_i) \geq 0$  and  $\bar{l}_i \leq l_{i,2}$ , and (g) follows the fact that  $P_{d,i}(d_r)$  is a monotonically decreasing function on  $(l_{i,1}, l_{i,2})$ .

**Theorem 1:** The detection probability at detection distance  $d_r$  in sector  $i \in \{1, 2, ..., N+1\}$ ,  $P_{d,i}(d_r)$ , is given by

$$P_{d,i}(d_r) \approx \sum_{k=1}^{m} {m \choose k} (-1)^{k+1} \frac{\mathcal{L}_{I_{r,i}}(k\xi T_{r,i}(d_r))}{\exp(k\xi T_{r,i}(d_r)N_0 B)}$$
(22)

where  $\xi = (m!)^{-\frac{1}{m}}$  and  $T_{\mathrm{r},i}(d_{\mathrm{r}}) = m\gamma_{\mathrm{r}}/(P_{\mathrm{r}}(i)L_{\mathrm{ref}}(d_{\mathrm{r}},d_{\mathrm{r}}))$ . Proof: One can calculate  $P_{\mathrm{d},i}(d_{\mathrm{r}})$  as follows

$$P_{d,i}(d_{r}) = \mathbb{P}\left\{h_{\mathbf{x}_{\text{TV}},\mathbf{x}_{\text{TA}}} \geq \frac{T_{r,i}(d_{r})J_{r,i}}{m}\right\}$$

$$\stackrel{\text{(h)}}{=} 1 - \mathbb{E}_{J_{r,i}}\left[\frac{\Gamma_{L}(m, T_{r,i}(d_{r})J_{r,i})}{\Gamma(m)}\right]$$

$$\stackrel{\text{(i)}}{\approx} \sum_{k=1}^{m} \binom{m}{k} (-1)^{k+1} \frac{\mathcal{L}_{I_{r,i}}(k\xi T_{r,i}(d_{r}))}{\exp(k\xi T_{r,i}(d_{r})N_{0}B)}$$
(23)

where  $J_{r,i} = I_{r,i} + N_0 B$ , (h) is from the CDF of the channel gain, and (i) follows Appendix G in [13].

As  $\mathcal{L}_{I_{\mathrm{r},i}}(k\xi T_{\mathrm{r},i}(d_{\mathrm{r}}))$  depends on  $P_{\mathrm{d},i}$ , which generates difficulty to find  $P_{\mathrm{d},i}(d_{\mathrm{r}})$  directly, in this work, we replace  $P_{\mathrm{d},i}$  with its lower bound to calculate  $P_{\mathrm{d},i}(d_{\mathrm{r}})$ .

### B. Communication Coverage Probability

Next, we study the communication coverage probability [12], defined as the probability that the SINR of the communication signal received by the TV is no less than the communication SINR threshold  $\gamma_c$ . Then, the communication coverage probability at communication distance  $d_c$  in sector i,  $P_{c,i}(d_c)$ , can be defined as

$$P_{c,i}(d_c) = \mathbb{P}\left\{\frac{S_{c,i}(d_c)}{I_{c,i} + N_0 B} \ge \gamma_c\right\}$$
(24)

where  $I_{\mathrm{c},i} = I_{1,i}^{\mathrm{inc}} + \sum_{k'=1}^{3} I_{k',i}^{\mathrm{ref}}$  is the total power of interference signals received at the communication receiver in sector i.

**Theorem 2:** The communication coverage probability at communication distance  $d_c$  in sector  $i \in \{1, 2, ..., N+1\}$ ,  $P_c(d_c)$ , is given by

$$P_{c,i}(d_c) \approx \sum_{k=1}^{m} \binom{m}{k} (-1)^{k+1} \frac{\mathcal{L}_{I_{c,i}}(k\xi T_{c,i}(d_c))}{\exp[k\xi T_{c,i}(d_c)N_0 B]}$$
 where  $T_{c,i}(d_c) = m\gamma_c/(P_c(i)L_{\text{inc}}(d_c))$ . (25)

*Proof*: Theorem 2 can be proved similar to Theorem 1. ■

It is noteworthy that, to avoid complex numerical calculation, we can use the lower bound of  $P_{d,i}$  in deriving  $P_{c,i}(d_c)$ .

### C. ISAC Performance Optimization

In the proposed ISAC framework, the total system power  $P_t$  should be properly allocated between radar and communication to maximize the detection probability while guaranteeing communication performance. Typically, the optimization problem (OP) can be formulated in the following two forms.

Comprehensiveness: One can maximize the average detection probability of N+1 sectors at the required maximum

TABLE I SIMULATION PARAMETER SETTINGS

Symbol	Value	Symbol	Value	Symbol	Value
θ	15°	B	100 MHz	$f_c$	28 GHz
$P_t$	10 W	$N_0$	-174 dBm/Hz	l	10 m
$P_{\rm rf}/P_{\rm rs}$	8 W	β	0.6	$\gamma_{ m r}$	0 dB
$P_{\rm c}$	2 W	σ	10 dBsm	$\gamma_{ m c}$	20 dB
$G_{ m T}/G_{ m R}$	16	α	2.2	$l_{ m f}$	120 m
$d_{ m h}$	10 m	m	3	$l_{ m s}$	75 m

detection distance, for which the power allocation problem can be formulated as

$$\max_{P_{\rm rf}, P_{\rm rs}} \frac{1}{N+1} \sum_{i=1}^{N+1} P_{\rm d,}i(d_{\max,i})$$
 (26)

s.t. 
$$P_{c,i}(d_{\max,i}) \ge \beta, i = 1, 2, \dots, N+1,$$
 (26a)

$$P_{\rm rf} + P_{\rm c} = P_t, \tag{26b}$$

$$0 \le P_{\rm rs} \le P_{\rm rf},\tag{26c}$$

where  $\beta$  is the threshold of communication coverage probability,  $P_{\mathrm{d},i}(d_{\mathrm{max},i})$   $(P_{\mathrm{c},i}(d_{\mathrm{max},i}))$  is the detection (communication coverage) probability of sector i at the required maximum detection distance  $d_{\mathrm{max},i}$ . Here, we consider that  $d_{\mathrm{max},i} = \sqrt{\max(|s_{i,1}|,|s_{i,2}|)^2 + l^2}$  for  $i \in \{2,3,...,N\},$   $d_{\mathrm{max},1} = l_{\mathrm{f}},$  and  $d_{\mathrm{max},N+1} = l_{\mathrm{s}},$  where  $l_{\mathrm{f}}$  and  $l_{\mathrm{s}}$  are preset constants. Constraint (26a) ensures the communication quality of each sector, (26b) gives the total power budget, and (26c) is to improve the safety of the front radar.

Fairness: Another is maximizing the minimum detection probability of N+1 sectors to ensure fairness, and then the power allocation problem can be expressed as

$$\max_{P_{\rm rf}, P_{\rm rs}} \quad \min\{P_{\rm d,1}(d_{\rm max,1}), ..., P_{\rm d,N+1}(d_{\rm max,N+1})\}$$
 s.t. (26a), (26b), and (26c).

Because of the complicated analytical expressions under 1D MHCP, the OPs in (26) and (27) can hardly be directly solved. So, we solve the OPs by using exhaustive search.

# V. PERFORMANCE EVALUATION

In this section, Monte Carlo simulations are conducted to validate the analytical results and study the impact of power allocation. We consider a 10 km-long straight segment for a dual-direction and two-lane scenario, and the vehicles with a speed of 60 km/h are dropped according to 1D MHCP. The simulation is repeated at least 5,000 times, and the granularity of the exhaustive search is 0.25W. Unless otherwise stated, the simulation parameters are given in Table I [5, 8, 9, 14].

Fig. 4 shows the radar (communication) performance of each sector versus the distance between the TV and the TA (CV), under different probabilities of spectrum resource collision  $\varepsilon$  and vehicle densities  $\lambda_{\rm p}$ . One can observe from the figures that the analytical results match with the simulation results. It can also be seen from the figure that the reflected interference is not negligible. As compared with the CCP, the DP is more susceptible to reflected interference. Further, the reflected interference has a greater impact on the performance of the side direction from the directional perspective. For the radar performance of each sector, it is observed from Fig. 4(a) that the front DP remains greater than 0.9 when the distance between the TV and the TA is less than 110 m, at  $\lambda_{\rm p}=0.01$  cars/m and  $\varepsilon=0.01$ . The DP of the side direction shown in Fig. 4(c) exceeds 0.9 even under  $\lambda_{\rm p}=0.1$  cars/m and

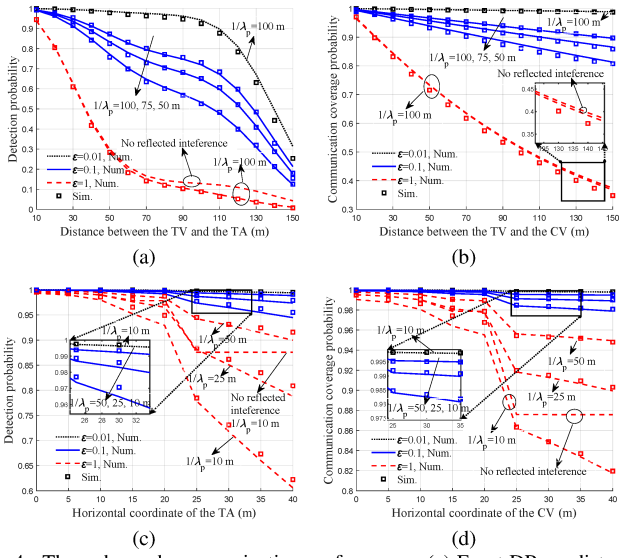


Fig. 4. The radar and communication performance: (a) Front DP vs. distance between the TV and the TA; (b) Front CCP vs. distance between the TV and the CV; (c) Side DP vs. horizontal coordinate of the TA; (d) Side CCP vs. horizontal coordinate of the CV.

 $\varepsilon=0.1.$  As compared with the side DP, the front DP decreases more sharply with the growth of  $\lambda_{\rm p}$  and  $\varepsilon$  due to more signal interference suffered. For communication performance, thanks to the low path loss of incident signals, the CCP of the front direction in Fig. 4(b) can remain higher than 0.8 even at 150 m except for  $\varepsilon=1$ , and the minimum of side CCP in Fig. 4(d) is about 0.82. The simulation results of the backward direction are similar to those of the forward direction, thus omitted for space limitation. From the simulation results, we find that the radio resources of the network need to be allocated rationally to alleviate spectrum resource collision, especially under severe traffic (i.e.,  $\lambda_{\rm p} d_{\rm h} \geq 1$ ) and scarce radio resources (i.e.,  $\varepsilon \geq 0.1$ ).

Fig. 5 studies the impact of optimizing power allocation. The performance of the proposed schemes is compared with a heuristic power allocation scheme, in which the power of radar signals is allocated according to  $d_{\max,i}$ , i.e.,  $P_{\rm r}(i) \propto$  $d_{\max,i}^{-2\alpha} P_t$ . Specifically, Fig. 5(a) shows the average DP versus vehicle density  $\lambda_{\rm p}$ , and Fig. 5(b) shows the relationship between the DP of TV in each sector and  $\lambda_{\rm p}$ . As shown in Fig. 5(a), it is obvious that scheme Comprehensiveness is the best, and scheme Fairness performs slightly worse than Comprehensiveness but has a huge improvement as compared to scheme Heuristic. It is shown in Fig. 5(b) that, the DP of scheme Heuristic is the smallest in most sectors, while scheme Comprehensiveness is the opposite, generating the huge performance gap between them as shown in Fig. 5(a). From Fig. 5(b), we can also observe that, scheme Fairness improves the DP of sector 1 by sacrificing the performance of other sectors, as described by the objective function in (27).

# VI. CONCLUSION

In this paper, a dual-beam ISAC scheme allowing 360° radar detection has been designed for vehicular networks. To analyze the performance of the ISAC networks, we have studied two cases of incident interference and three cases of

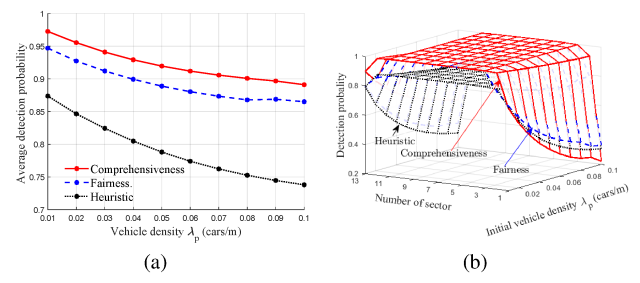


Fig. 5. Comparison of three power allocation schemes: (a) Average DP vs.  $\lambda_{\rm p}$ ; (b) DP of each sector vs  $\lambda_{\rm p}$ , with  $\varepsilon=0.05$ .

reflected interference in a dual-direction and two-lane scenario. Further, stochastic geometry has been applied to study the performance of the ISAC vehicular networks. Then, we have studied the power allocation between radar and communication among different sectors to optimize the performance of the ISAC networks. Simulation results not only verify that the reflected interference is not negligible and the radio resources of the network need to be allocated rationally to alleviate spectrum resource collision, but also show the effectiveness of the proposed power allocation schemes in improving the average detection probability of 360° radar.

#### REFERENCES

- J. A. Zhang et al., "Enabling joint communication and radar sensing in mobile networks—a survey," *IEEE Commun. Surveys Tuts.*, vol. 24, no. 1, pp. 306–345, Oct. 2021.
- [2] Q. Zhang, X. Wang, Z. Li, and Z. Wei, "Design and performance evaluation of joint sensing and communication integrated system for 5G mmwave enabled CAVs," *IEEE J. Sel. Topics Signal Process.*, vol. 15, no. 6, pp. 1500–1514, Nov. 2021.
- [3] S. Bartoletti et al., "Sidelink 5G-V2X for integrated sensing and communication: The impact of resource allocation," in Proc. IEEE/CIC Int. Conf. Commun.(ICC Workshops), pp. 79–84, 2022.
- [4] S. H. Dokhanchi, B. S. Mysore, K. V. Mishra, and B. Ottersten, "A mmWave automotive joint radar-communications system," *IEEE Trans. Aerosp. Electron. Syst.*, vol. 55, no. 3, pp. 1241–1260, Jun. 2019.
- [5] R. Singh et al., "R-comm: A traffic based approach for joint vehicular radar-communication," *IEEE Trans. Intell. Veh.*, vol. 7, no. 1, pp. 83–92, Mar. 2022
- [6] L. Pucci, E. Paolini, and A. Giorgetti, "System-level analysis of joint sensing and communication based on 5G new radio," *IEEE J. Sel. Areas Commun.*, vol. 40, no. 7, pp. 2043–2055, Jul. 2022.
- [7] W. Yi, Y. Liu, and A. Nallanathan, "Signal fractions analysis and safety-distance modeling in V2V inter-lane communications," *IEEE Commun. Lett.*, vol. 25, no. 4, pp. 1387–1390, Apr. 2021.
- [8] W. Yi et al., "Modeling and analysis of mmwave V2X networks with vehicular platoon systems," *IEEE J. Sel. Areas Commun.*, vol. 37, no. 12, pp. 2851–2866, Dec. 2019.
- [9] A. Al-Hourani et al., "Stochastic geometry methods for modeling automotive radar interference," *IEEE Trans. Intell. Transp. Syst.*, vol. 19, no. 2, pp. 333–344, Feb. 2018.
- [10] G. Ghatak, S. S. Kalamkar, and Y. Gupta, "Radar detection in vehicular networks: Fine-grained analysis and optimal channel access," *IEEE Trans. Veh. Technol.*, vol. 71, no. 6, pp. 6671–6681, Jun. 2022.
- [11] Y. Wang et al., "Performance analysis of uncoordinated interference mitigation for automotive radar," *IEEE Trans. Veh. Technol.*, vol. 72, no. 4, pp. 4222–4235, Apr. 2023.
- [12] F. D. S. Moulin, C. Wiame, L. Vandendorpe, and C. Oestges, "Joint performance metrics for integrated sensing and communication systems in automotive scenarios," arXiv preprint arXiv:2208.12790, Aug. 2022.
- [13] M. Matracia, M. A. Kishk, and M.-S. Alouini, "UAV-aided post-disaster cellular networks: A novel stochastic geometry approach," *IEEE Trans. Veh. Technol.*, vol. 72, no. 7, pp. 9406–9418, Jul. 2023.
- [14] H. Liang et al., "Extending 5G NR V2X mode 2 to enable integrated sensing and communication for vehicular networks," in Proc. IEEE/CIC Int. Conf. Commun. China (ICCC Workshops), pp. 1–6, Aug. 2023.